ACS OMEGA

http://pubs.acs.org/journal/acsodf

Article

Theoretical Prediction of Rhenium Separation from Ammonium Perrhenate by Phonon−Photon Resonance Absorption

Miao-Miao Li, Jing-Wen Cao, Xiao-Ling Qin, Xiao-Yan Liu, Xiao-Qing Yuan, Xiao-Tong Dong, Qing Guo, Yi Sun, and Peng Zhang*

Cite This: *ACS Omega* 2022, 7, 5437−5441

Read Online

ACCESS | Metrics & More | Article Recommendations | Supporting Information

ABSTRACT: Rhenium (Re) is an extremely rare and precious element that is mainly used in the construction of aerospace components and satellite stations. However, an efficient and simple method for preparing Re has yet to be devised. To this end, we investigated the vibrational spectrum of ammonium perrhenate (NH_4ReO_4) using the CASTEP code based on first-principles density functional theory. We assigned the infrared (IR) absorption and Raman scattering spectra for NH_4ReO_4 using a dynamic process analysis of optical branch normal modes. We examined the IR-active peaks of Re-related vibrational modes in detail and found that the typical IR peak at approximately 914 cm^{-1} is due to the Re−O bond stretching. Thus, we posit that strong terahertz laser irradiation of NH_4ReO_4 at 914 cm^{-1} will lead to sufficient resonance absorption to cleave its Re−O bonds. This method could potentially be used to efficiently separate Re from its oxides.

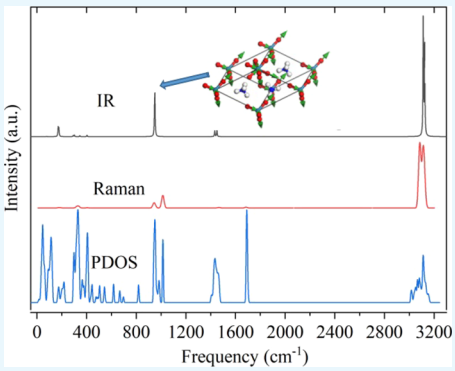

INTRODUCTION

Rhenium (Re) is an extremely rare and precious element with high melting and boiling points. It is also the only refractory metallic element that does not react with carbon.[1−4] Consequently, Re has important applications in petroleum and aerospace industries. It is mostly used in the form of superalloys (78%), with the remainder used in catalysts (14%) and other applications (8%).[5] Thus, Re superalloys are critical constituents of aerospace components and satellite stations. For example, the Re−nickel superalloy is the core material of modern jet engines, turbine disks, and other important structural components.[6−9] Moreover, the core components of the engine of China's first Mars probe, "Tianwen-1," are made of the Re superalloy. The world's demand for Re has therefore increased dramatically in recent years, and the mining and recovery of Re resources are of great strategic importance to many countries worldwide.

At present, the separation of Re from other metals and oxides in aqueous solution is an important step in the production of Re from ores and secondary raw materials and is performed by solvent extraction[10−16] or ion exchange.[17−19] This is followed by a high-temperature reduction and a complex deoxidation process, for which high-temperature-resistant equipment is required. An efficient and simpler method for the isolation of Re has yet to be developed.[20] There has also been a lack of research on the recovery of Re from secondary resources such as waste catalysts and waste alloys. Thus, there is a need for the development of such recovery technologies that are suitable for large-scale and industrial applications, and continued research in this area is crucial for ensuring future demand for Re can be met.[21]

Many spectroscopic studies have focused on ammonium perrhenate (NH_4ReO_4),[22−31] which is the most common commercial form of Re. Korppi-Tommola et al., for example, examined the temperature dependence of the Raman spectrum of NH_4ReO_4.[23] In a related work, Gassman et al. fabricated sodium borosilicate sunglasses containing Re and used confocal Raman microscopy to study their vibrational spectra. This showed that the spectra of ReO_4^- exhibited different Raman bands to those of persulfate.[28] Borowiec et al. obtained the Raman spectrum of NH_4ReO_4, which they sulfated at room temperature to form Re disulfide.[29] Brown et al. studied the lattice structure of NH_4ReO_4—specifically, the thermal contraction of the *a*-lattice parameter and the substantial thermal expansion of the *c*-lattice parameter—and the enhanced nuclear quadrupole relaxation and increased specific heat capacity of NH_4ReO_4.[30,31]

However, despite the above experimental and computational studies of NH_4ReO_4, there is a dearth of theoretical methods for the assignment of peaks in NH_4ReO_4 spectra. Thus, in this study, we simulated the vibrational spectra of NH_4ReO_4 and used normal mode analysis to identify the Re-related peaks.

Received: November 29, 2021
Accepted: January 25, 2022
Published: February 2, 2022

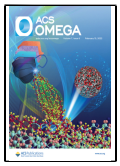

Our identification of the Re-related vibrational peaks allowed us to determine the IR-active modes of Re in previously reported experimentally obtained spectra of NH_4ReO_4. Based on these findings, we propose a novel method for the separation of Re from its oxides that exploits photon−phonon resonance absorption.

METHODS

We used the CASTEP code for geometric optimization and phonon calculations, based on first-principles density functional theory.[32] Due to the large change in the gradient of electron density in NH_4ReO_4, we employed the generalized gradient approximation of the Perdew−Burke−Ernzerhof exchange−correlation functional.[33] The convergence tolerance value of the energy and self-consistent field was set to 1×10^{-9} eV/atom. The energy cutoff was set to 830 eV and a $3 \times 3 \times 3$ *k*-point mesh was used. The norm-conserving pseudo-potential was applied to calculate the phonons via the linear response method, and IR and Raman intensity calculations were also performed. Thus, we obtained simulated IR and Raman spectra that were suitable for comparison with spectral data previously reported by others, thereby enabling us to assign Re-related peaks in these spectra via a dynamic process analysis of each normal-mode vibration.

RESULTS AND DISCUSSION

NH_4ReO_4 crystallizes with the Scheelite ($CaWO_2$) structure. Its space group is $I4_1/a$, with two formula units per primitive cell.[25,34] According to the group theory, both ReO_4^- and NH_4^+ occupy S_4 sites, with N and Re in Wyckoff positions *a* and *b*, respectively, and O and H atoms occupying general Wyckoff *f* positions. A factor group analysis of NH_4ReO_4 was made using Adams' tables.[35] The 60 vibrational normal modes of NH_4ReO_4 are classified as $4A_g + 6B_g + 4E_g + 6A_u + 4B_u + 4E_u$ internal modes, $2A_g + 2B_g + 4E_g + A_u + 2B_u + 3E_u$ external modes, and $A_u + E_u$ acoustic modes.[23] As both ReO_4^- and NH_4^+ occupy S_4 sites in the lattice, their modal analyses are the same: each pair of identical ions gives rise to $2A_g + 3B_g + 2E_g + 3A_u + 2B_u + 2E_u$ internal modes in the primitive cell. These can be correlated to the "free" ion vibrations ν_1 (A_l), ν_2 (E), ν_3, and ν_4 (F_2).[36] Accordingly, in the Raman spectrum of crystalline NH_4ReO_4, the A_1 mode of the "free" ion should remain a singlet, while the E and F_2 modes should be split into doublets. The external optical modes are classified as rotatory (or librational) (ν_L) lattice modes or translational (ν_T) lattice modes. Given the substantial difference between the ionic masses of NH_4^+ and ReO_4^-, it is reasonable to separate the external modes into two groups describing the motions of the two ions. The rotational and translational motions of a "free" ion of symmetry T_d represent those of species F_1 and F_2.

Figure 1 shows simulated IR, Raman, and phonon density of states (PDOS) spectra of NH_4ReO_4. Based on the harmonic approximation, there are 57 optical branch lattice waves ($20 \times 3 - 3$) for a 20-molecular primitive cell. That is, there are fewer than 57 normal-mode phonon−photon couplings with IR light. Due to the special symmetry of NH_4ReO_4, its IR- and Raman-active modes are complementary, as shown in Table 1. Korppi-Tommola et al. reported the Raman spectrum of NH_4ReO_4 in 1978 and assigned the peaks by comparing the vibrational peaks of NH_4ReO_4 and ND_4ReO_4. They concluded that the peaks at 49, 67, 120, and 135 cm^{-1}, which are not affected by deuteration, are mainly caused by the vibrations of

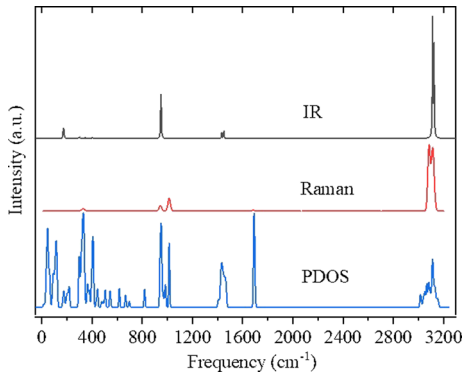

Figure 1. Simulated vibrational spectra of ammonium perrhenate: IR spectrum (black), Raman spectrum (red), and PDOS (blue).

ReO_4^-. In addition, they found that the peaks at 49 and 67 cm^{-1} are ion-cluster ν_T modes, whereas the peaks at 120 and 135 cm^{-1} are ν_L modes.[23] Park et al. measured the Raman spectrum of $^{15}NH_4ReO_4$, within which they identified two sets of ReO_4^- vibrational peaks (50/69 and 122/144 cm^{-1}).[37] Our simulations identified six Raman-active modes at similar frequencies to those above: 47(2), 54, 107(2), and 120 cm^{-1}. We performed dynamic process analysis that revealed that three of these modes [47(2) and 54 cm^{-1}] represent translational motions of ions between different NH_4^+ and ReO_4^- ion clusters. We also identified two IR-active degenerate modes at 79 cm^{-1}, and a Raman- and IR-inactive mode at 128 cm^{-1}. The six modes 79(2), 107(2), 120, and 128 cm^{-1} are primarily librational modes of ReO_4^- clusters. Two typical modes (47 and 120 cm^{-1}) are shown in Figure 2.

Thompson et al. studied the vibrational spectra of NH_4ReO_4 and the double complex salt $Pd(NH_3)_4(ReO_4)_2$. They proposed that the vibrational modes in the low-frequency region from 100 to 600 cm^{-1} are attributable to skeletal vibration modes, whereas those in the higher frequency region (600−1200 cm^{-1}) are primarily ReO_4^- vibrations.[38] Tommola et al. assigned the peaks of NH_4ReO_4 at 189 and 210 cm^{-1} to ν_T. Park et al. identified the Raman spectral peaks of NH_4ReO_4 at 191 and 214 cm^{-1}.[37] According to our work, the normal modes at 170(2) and 177 cm^{-1} are IR-active, whereas the normal modes at 176(2) and 189 cm^{-1} are Raman-active and that all of these normal modes are translational modes of NH_4^+.

Thompson et al. reported an NH_4ReO_4 IR spectral peak at approximately 290 cm^{-1}, which they attributed to the O−Re−O bending.[38] Korppi-Tommola et al. assigned an NH_4ReO_4 Raman spectral peak at 264 cm^{-1} to ν_L.[23] Park et al. found two Raman spectral peaks (at 265 and 276 cm^{-1}).[37] According to Table 1, 10 modes from 292 to 345 cm^{-1} correspond to ReO_4^- librational modes. In contrast, six modes [at 403(2), 404, 405(2), and 413 cm^{-1}] are librations of NH_4^+. See one example at 404 cm^{-1} in Figure 3.

Korppi-Tommola et al. suggested that the Raman spectral peaks at 893 and 910 cm^{-1} are associated with a ReO_4^- $\nu_3(F_2)$ vibration mode.[23] Similarly, Thompson attributed the strong IR spectral peak at 914 cm^{-1} to antisymmetric Re−O stretching.[38] Gonzalez-Rodriguez deduced that the IR spectral peak at 913 cm^{-1} was related to ReO_4^- by comparing the IR spectra of NH_4ReO_4 and potassium perrhenate ($KReO_4$).[39] Moreover, this peak is very close to the peak at 910 cm^{-1} for ReO_4^- in the IR spectrum of the $[(CuCl)_3L](PF_6)(ReO_4)_2 \cdot 3H_2O$ complex, which was obtained by Cao.[10] In the current

https://doi.org/10.1021/acsomega.1c06744
ACS Omega 2022, 7, 5437−5441

Table 1. Comparison of Calculated Raman- or IR-Active Normal Modes for NH_4ReO_4 (the Number in Brackets in the First Column Indicates the Degeneracy) with Reported Raman and Infrared (IR) Spectroscopy Data (cm^{-1})

	Raman		IR		
normal modes	ref 23	ref 37	ref 38	ref 39	vibrational mode
47(2) Raman	49	50			skeletal translation
54 Raman	67	69			skeletal translation
79(2) IR					ReO_4^- libration
107(2) Raman	120	122			ReO_4^- libration
120 Raman	135	140			ReO_4^- libration
128					ReO_4^- libration
170(2) IR					NH_4^+ translation
176(2) Raman	189	191			NH_4^+ translation
177 IR					NH_4^+ translation
189 Raman	210	214			NH_4^+ translation
292 IR			290		ReO_4^- bending
301(2) IR					ReO_4^- bending
318 Raman	263	265			ReO_4^- bending
320 Raman	328	276			ReO_4^- bending
329(2) Raman	335				ReO_4^- bending
337 Raman	351				ReO_4^- bending
339					ReO_4^- bending
345 IR					ReO_4^- bending
403(2) IR					NH_4^+ libration
404 Raman					NH_4^+ libration
405(2) Raman					NH_4^+ libration
413					NH_4^+ libration
942(2) Raman	893				ReO_4^- stretching
947 IR			914	913	ReO_4^- stretching
950(2) IR					ReO_4^- stretching
952 Raman	910				ReO_4^- stretching
1014 Raman	969				ReO_4^- stretching
1015					ReO_4^- stretching
1432(2) IR			1450	1448	NH_4^+ bending
1450 IR					NH_4^+ bending
1451(2) Raman	1431	1433			NH_4^+ bending
1468 Raman	1438	1440			NH_4^+ bending
1684 Raman	1658	1658			NH_4^+ bending
1687 Raman					NH_4^+ bending
1692 IR					NH_4^+ bending
1704					NH_4^+ bending
3084					NH_4^+ stretching
3085 Raman	3128	3130			NH_4^+ stretching
3112(2) Raman					NH_4^+ stretching
3113(2) IR					NH_4^+ stretching
3123 Raman	3182	3182			NH_4^+ stretching
3124 IR			3225	3150	NH_4^+ stretching

study of NH_4ReO_4, we identified these NH_4ReO_4 peaks at similar frequencies to those above: four Raman-active modes [942(2), 952, and 1014 cm^{-1}], three IR-active modes [947 and 950(2)] cm^{-1}, and one IR- and Raman-inactive mode at 1015 cm^{-1} (Table 1). Our dynamic analysis confirmed that these eight modes are all related to Re−O stretching.

The IR-active mode at 947 cm^{-1} corresponds to the experimental IR peak at around 914 cm^{-1}. The dynamic process of Re−O antisymmetric stretching at 947 cm^{-1} can be seen from the Supporting Information file. Interestingly, while this mode shows the second intensity in the simulated spectrum, the experiments from refs 38 and 39 presented that this peak shows the highest intensity in the IR spectrum.

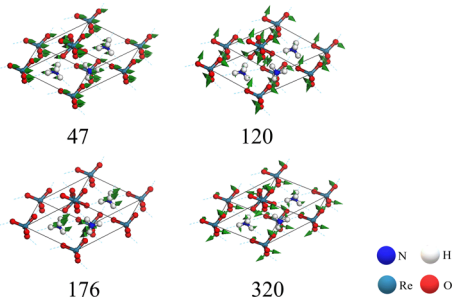

Figure 2. Four examples of vibrational modes of ammonium perrhenate in the region from 47 to 345 cm^{-1}. The green arrows represent the direction of vibration, which is proportional to the amplitude of the vibration. The number below each mode indicates its wavenumber.

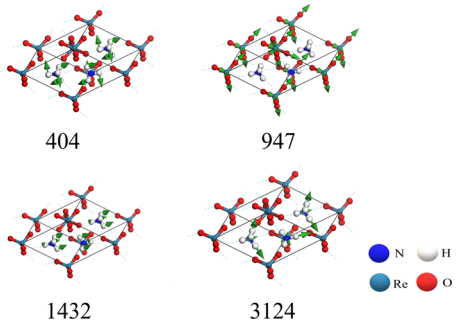

Figure 3. Four examples of vibrational modes of ammonium perrhenate in the region from 403 to 3124 cm^{-1}. The green arrows represent the direction of vibration, which is proportional to the amplitude of the vibration. The number below each mode indicates its corresponding wavenumber.

That means, the phonon−photon resonance absorption at this peak is highly efficient. Provided a terahertz laser at this frequency be supplied to NH_4ReO_4, the direct energy absorption of the Re−O bond will result in energy level transitions and facilitate the Rhenium separation from NH_4ReO_4.

In the higher energy region from 1432 to 3124 cm^{-1}, we found that all of the vibrational modes are related to NH_4^+ clusters, due to the lower mass of this ion.

Gonzalez-Rodriguez et al. also compared the IR spectra of NH_4ReO_4 and $KReO_4$. This revealed that the peaks present in both spectra correspond to ReO_4^- and that the peaks of NH_4ReO_4 at frequencies from 1448 to 3304 cm^{-1} are those for NH_4^+.[39] Similarly, Devarajan et al. observed two Raman peaks—at 1438 and 3182 cm^{-1}—for NH_4ReO_4, which they assigned to v_3 (F_2) stretching and v_4 (F_2) bending modes, respectively, of NH_4^+.[40] Thompson[38] and Gonzalez-Rodriguez[39] observed an IR spectrum peak for NH_4ReO_4 at approximately 1450 and 1448 cm^{-1}, respectively. Korppi-Tommola et al. observed Raman spectrum peaks for NH_4ReO_4 at 1431, 1438, and 1658 cm^{-1},[23] and Park et al. observed Raman spectrum peaks for NH_4ReO_4 at 1433, 1440, and 1658 cm^{-1}.[37] In our simulations, 10 modes in the region from 1432 to 1704 cm^{-1} represent bending vibrations of NH_4^+ ions.

At frequencies above 3000 cm^{-1}, several distinct vibrational peaks can be seen in both the IR and Raman spectra of NH_4ReO_4, which correspond to the stretching vibrations of the N−H bond of NH_4^+. Korppi-Tommola et al.[23] found a Raman spectrum peak at 3128 cm^{-1}, while Park et al.[37] found a Raman

https://doi.org/10.1021/acsomega.1c06744
ACS Omega 2022, 7, 5437−5441

spectrum peak at 3130 cm^{-1}, which they assigned to v_1 (A_1), and also found a Raman peak at 3182 cm^{-1}, which they assigned to v_3 (F). Thompson et al.[38] observed a significant IR spectrum peak at 3225 cm^{-1} and Gonzalez-Rodriguez et al.[39] observed an IR peak at 3150 cm^{-1}. In our work, these eight modes represent various N−H stretching modes. For example, see the vibrational mode at 3124 cm^{-1}, as shown in Figure 3.

CONCLUSIONS

We calculated the normal modes of NH_4ReO_4 and performed a dynamic process analysis of the calculated modes, which revealed that the compound forms two ion clusters that vibrate almost independently. In the lowest frequency region, three modes from 47 to 54 cm^{-1} are skeletal deformations, in which all of the ion clusters exhibit translational motions. Next, those from 79 to 128 cm^{-1} are mainly ReO_4^- librations, whereas those from 170 to 189 cm^{-1} are vibrational modes related to translational motions of NH_4^+. The next bands of modes, from 292 to 345 cm^{-1}, are various bending modes of ReO_4^-, whereas those from 403 to 413 cm^{-1} are vibrational modes representing all of the possible NH_4^+ rotations. In the two high-energy bands from 1432 to 3124 cm^{-1}, all of the modes represent NH_4^+ bending and stretching vibrations. Each vibrational mode is unique, and the degenerate modes have different vibrational directions.

We confirmed that the modes from 942 to 1015 cm^{-1} represent O−Re stretching; the significant IR spectrum peaks at approximately 914 cm^{-1} represent one kind of O−Re stretching. The Supporting Information Video shows the dynamic process of the O−Re stretching. The IR-active vibrational mode is high-intensity, which means that this mode resonantly absorbs a large amount of IR radiation.

Re is present in molybdenum and copper ores and is produced commercially as a byproduct of the metallurgical processing of these ores. Specifically, the Re in the ores is the Re_2O_7 powder, which is subsequently dissolved in aqueous solution to form ReO_4^-.[16,41,42] As mentioned, two chemical methods used for the extraction of Re are solvent extraction[10−16] and ion exchange,[17−19] and these are currently used in industrial processes.[41,43] Our findings suggest that a strong terahertz laser irradiation of ReO_4^- at 914 cm^{-1} may result in resonance absorption sufficient to cleave its Re−O bonds, thereby facilitating the separation of Re.

ASSOCIATED CONTENT

Supporting Information

The Supporting Information is available free of charge at https://pubs.acs.org/doi/10.1021/acsomega.1c06744.

Vibration mode of NH_4ReO_4 at 914 cm^{-1} (MP4)

AUTHOR INFORMATION

Corresponding Author

Peng Zhang − *School of Space Science and Physics, Shandong University, Weihai 264209, China;* orcid.org/0000-0002-1099-6310; Email: zhangpeng@sdu.edu.cn

Authors

Miao-Miao Li − *School of Space Science and Physics, Shandong University, Weihai 264209, China; SDU-ANU Joint Science College, Shandong University, Weihai 264209 Shandong, China*

Jing-Wen Cao − *School of Space Science and Physics, Shandong University, Weihai 264209, China;* orcid.org/0000-0002-3226-3281

Xiao-Ling Qin − *School of Space Science and Physics, Shandong University, Weihai 264209, China*

Xiao-Yan Liu − *School of Space Science and Physics, Shandong University, Weihai 264209, China*

Xiao-Qing Yuan − *School of Space Science and Physics, Shandong University, Weihai 264209, China*

Xiao-Tong Dong − *School of Space Science and Physics, Shandong University, Weihai 264209, China*

Qing Guo − *School of Space Science and Physics, Shandong University, Weihai 264209, China; SDU-ANU Joint Science College, Shandong University, Weihai 264209 Shandong, China*

Yi Sun − *School of Space Science and Physics, Shandong University, Weihai 264209, China*

Complete contact information is available at: https://pubs.acs.org/10.1021/acsomega.1c06744

Notes

The authors declare no competing financial interest.

ACKNOWLEDGMENTS

We are grateful to the National Natural Science Foundation of China for financial support (grant no. 11075094). The numerical calculations were performed on the supercomputing system at the Supercomputing Center, Shandong University, Weihai.

REFERENCES

(1) Hori, H.; Otsu, T.; Yasukawa, T.; Morita, R.; Ishii, S.; Asai, T. Recovery of rhenium from aqueous mixed metal solutions by selective precipitation: a photochemical approach. *Hydrometallurgy* **2019**, *183*, 151−158.

(2) Dilworth, J. R. Rhenium chemistry−then and now. Coord. *Chem. Rev.* **2021**, *436*, 213822.

(3) Tzvetkova, C.; Novo, L. A. B.; Atanasova-Vladimirova, S.; Vassilev, T. On the uptake of rhenium by plants: Accumulation and recovery from plant tissue. *J. Cleaner Prod.* **2021**, *328*, 129534.

(4) Fridkin, G.; Bonasera, T. A.; Litman, P.; Gilon, C. Backbone metal-cyclization: a novel approach for simultaneous peptide cyclization and radiolabeling. Application to the combinatorial synthesis of rhenium-cyclic somatostatin analogs. *Nucl. Med. Biol.* **2005**, *32*, 39−50.

(5) Blamey, A. Rhenium prices set to recover, aerospace key: Roskill. *Platts Metals Week* **2010**, *81*, 7.

(6) Chakravarty, R.; Shukla, R.; Tyagi, A. K.; Dash, A.; Venkatesh, M. Nanocrystalline zirconia: A novel sorbent for the preparation of $^{188}W/^{188}Re$ generator. *Appl. Radiat. Isot.* **2010**, *68*, 229−238.

(7) Singh Gaur, R. P.; Wolfe, T. A.; Braymiller, S. A. Recycling of rhenium-containing wire scrap. *Int. J. Refract. Met. Hard Mater.* **2015**, *50*, 79−85.

(8) Huang, Y.; Zhang, B.; Liu, B.; Su, S.; Han, G.; Wang, W.; Guo, H.; Cao, Y. Clean and deep separation of molybdenum and rhenium from ultra-low concentration solutions via vapidly stepwise selective coagulation and flocculation precipitation. *Sep. Purif. Technol.* **2021**, *267*, 118632.

(9) Okal, J.; Kępiński, L.; Krajczyk, L.; Tylus, W. Oxidation and redispersion of a low-loaded $Re/\gamma\text{-}Al_2O_3$ catalyst. *J. Catal.* **2003**, *219*, 362−371.

(10) Zhan-fang, C.; Hong, Z.; Qiu, Z. Solvent extraction of rhenium from molybdenum in alkaline solution. *Hydrometallurgy* **2009**, *97*, 153−157.

(11) Keshavarz Alamdari, E.; Darvishi, D.; Haghshenas, D. F.; Yousefi, N.; Sadrnezhaad, S. K. Separation of Re and Mo from roasting-dust leach-liquor using solvent extraction technique by TBP. *Sep. Purif. Technol.* **2012**, *86*, 143−148.
(12) Kang, J.; Kim, Y.-U.; Joo, S.-H.; Yoon, H.-S.; Rajesh Kumar, J.; Park, K.-H.; Parhi, P. K.; Shin, S. M. Behavior of extraction, stripping, and separation possibilities of rhenium and molybdenum from molybdenite roasting dust leaching solution using amine based extractant tri-otyl-amine (TOA). *Mater. Trans.* **2013**, *54*, 1209−1212.
(13) Khoshnevisan, A.; Yoozbashizadeh, H.; Mohammadi, M.; Abazarpoor, A.; Maarefvand, M. Separation of rhenium and molybdenum from molybdenite leach liquor by the solvent extraction method. *Miner. Metall. Process.* **2013**, *30*, 53−58.
(14) Lou, Z.; Guo, C.; Feng, X.; Zhang, S.; Xing, Z.; Shan, W.; Xiong, Y. Selective extraction and separation of Re(VII) from Mo(VI) by TritonX-100/N235/iso-amyl alcohol/n-heptane/NaCl microemulsion system. *Hydrometallurgy* **2015**, *157*, 199−206.
(15) Truong, H. T.; Nguyen, T. H.; Lee, M. S. Separation of molybdenum(VI), rhenium(VII), tungsten(VI), and vanadium(V) by solvent extraction. *Hydrometallurgy* **2017**, *171*, 28−305.
(16) Cheema, H. A.; Ilyas, S.; Masud, S.; Muhsan, M. A.; Mahmood, I.; Lee, J.-C. Selective recovery of rhenium from molybdenite flue-dust leach liquor using solvent extraction with TBP. *Sep. Purif. Technol.* **2018**, *191*, 116−121.
(17) Kholmogorov, A. G.; Kononova, O. N.; Kachin, S. V.; Ilyichev, S. N.; Kryuchkov, V. V.; Kalyakina, O. P.; Pashkov, G. L. Ion exchange recovery and concentration of rhenium from salt solutions. *Hydrometallurgy* **1999**, *51*, 19−35.
(18) Mozammel, M.; Sadrnezhaad, S. K.; Badami, E.; Ahmadi, E. Breakthrough curves for adsorption and elution of rhenium in a column ion exchange system. *Hydrometallurgy* **2007**, *85*, 17−23.
(19) Joo, S.-H.; Kim, Y.-U.; Kang, J.-G.; Kumar, J. R.; Yoon, H.-S.; Parhi, P. K.; Shin, S. M. Recovery of rhenium and molybdenum from molybdenite roasting dust leaching solution by ion exchange resins. *Mater. Trans.* **2012**, *53*, 2034−2037.
(20) Xiong, Y.; Xu, J.; Shan, W.; Lou, Z.; Fang, D.; Zang, S.; Han, G. A new approach for rhenium(VII) recovery by using modified brown algae Laminaria japonica adsorbent. *Bioresour. Technol.* **2013**, *127*, 464−472.
(21) Shen, L.; Tesfaye, F.; Li, X.; Lindberg, D.; Taskinen, P. Review of rhenium extraction and recycling technologies from primary and secondary resources. *Miner. Eng.* **2021**, *161*, 106719.
(22) Sharif Javaherian, S.; Aghajani, H.; Tavakoli, H. Investigation on ammonium perrhenate behaviour in nitrogen, argon and hydrogen atmosphere as a part of rhenium extraction process. *Miner. Process. Extr. Metall.* **2017**, *127*, 182−188.
(23) Korppi-Tommola, J.; Devarajan, V.; Brown, R. J. C.; Shurvell, H. F. The temperature dependence of the Raman spectrum of ammonium perrhenate. *J. Raman Spectrosc.* **1978**, *7*, 96−100.
(24) Johnson, R. A.; Rogers, M. T.; Leroi, G. E. Vibrational spectra of ammonium and other scheelite-type perrhenates. *J. Chem. Phys.* **1971**, *56*, 789−792.
(25) Gafurov, M. M.; Aliev, A. R. Molecular relaxation processes in the salt systems containing anions of various configurations. *Spectrochim. Acta, Part A* **2004**, *60*, 1549−1555.
(26) Brown, R. J. C.; Segel, S. L. ^{187}Re, ^{14}N, and ^{2}H nuclear quadrupole couplings in NH_4ReO_4: Evidence for a possible phase transition. *J. Chem. Phys.* **1977**, *67*, 3163−3169.
(27) Morrow, J. C. The crystal structure of $KReO_4$. *Acta Crystallogr.* **1960**, *13*, 443.
(28) Gassman, P. L.; McCloy, J. S.; Soderquist, C. Z.; Schweiger, M. J. Raman analysis of perrhenate and pertechnetate in alkali salts and borosilicate glasses. *J. Raman Spectrosc.* **2014**, *45*, 139−147.
(29) Borowiec, J.; Liang, W.; Boi, F. S.; He, Y.; Wang, S. L.; Gillin, W. P. Aluminium promoted sulfidation of ammonium perrhenate: presence of nanobattery in the ReS_2 composite material based memcapacitor. *Chem. Eng. J.* **2019**, *392*, 123745.
(30) Brown, R. J. C.; Callanan, J. E.; Weir, R. D.; Westrum, E. F., Jr The thermodynamics of ammonium scheelites. III. An analysis of the heat capacity and related data of deuterated ammonium perrhenate ND_4ReO_4. *J. Chem. Phys.* **1986**, *85*, 15.
(31) Brown, R. J. C.; Lynden-Bell, R. M. A computer simulation study of the disorder in ammonium per-rhenate. *J. Phys.: Condens. Matter* **1994**, *6*, 9903−9928.
(32) Clark, S. J.; Segall, M. D.; Pickard, C. J.; Hasnip, P. J.; Probert, M. I. J.; Refson, K.; Payne, M. C. First principles methods using CASTEP. *Z. Kristallogr.—Cryst. Mater.* **2005**, *220*, 567−570.
(33) Ernzerhof, M.; Scuseria, G. E. Assessment of the Perdew−Burke−Ernzerhof exchange-correlation func-tional. *J. Chem. Phys.* **1999**, *110*, 5029−5036.
(34) Oxton, I. A.; Knop, O.; Falk, M. Infrared spectra of the ammonium ion in crystals. II. The ammonium ion in trigonal environments, with a consideration of hydrogen bonding. *Can. J. Chem.* **1975**, *53*, 3394−3400.
(35) Adams, D. M. *Tables for Factor Group and Point Group Analysis*; Beckman-R11C Ltd: Newton, D. C., 1970.
(36) Johnson, R. A.; Rogers, M. T.; Leroi, G. E. Vibrational spectra of ammonium and other scheelite-type per-rhenates. *J. Chem. Phys.* **1972**, *56*, 789−792.
(37) Park, Y. S.; Shurvell, H. F.; Brown, R. J. C. The Raman spectrum of [^{15}N] ammonium perrhenate. *J. Raman Spectrosc.* **1986**, *17*, 351−354.
(38) Thompson, S. T.; Lamb, H. H.; Delley, B.; Franzen, S. Vibrational spectroscopy of the double complex salt $Pd(NH_3)_4(ReO_4)_2$, a bimetallic catalyst precursor. *Spectrochim. Acta, Part A* **2017**, *173*, 618−624.
(39) Gonzalez-Rodriguez, J.; Pepper, K.; Baron, M. G.; Mamo, S. K.; Simons, A. M. Production and analysis of recycled ammonium perrhenate from CMSX-4 superalloys. *Open Chem.* **2018**, *16*, 1298−1306.
(40) Korppi-Tommola, J.; Brown, R. J. C.; Shurvell, H. F.; Sala, O. The temperature dependence of the low frequency modes in the Raman spectra of ammonium per-rhenate and potassium perrhenate. *J. Raman Spectrosc.* **1981**, *11*, 363−368.
(41) Abisheva, Z. S.; Zagorodnyaya, A. N.; Bekturganov, N. S. Review of technologies for rhenium recovery from mineral raw materials in Kazakhstan. *Hydrometallurgy* **2011**, *109*, 1−8.
(42) Srivastava, R. R.; Lee, J.-c.; Kim, M.-s. Complexation chemistry in liquid−liquid extraction of rhenium. *J. Chem. Technol. Biotechnol.* **2015**, *90*, 1752−1764.
(43) Jia, M.; Cui, H.; Jin, W.; Zhu, L.; Liu, Y.; Chen, J. Adsorption and separation of rhenium(VII) using N-methylimidazolium functionalized strong basic anion exchange resin. *J. Chem. Technol. Biotechnol.* **2012**, *88*, 437−443.

https://doi.org/10.1021/acsomega.1c06744
ACS Omega 2022, 7, 5437−5441